



Water permeation through gas diffusion layers of proton exchange membrane fuel cells

A. Tamayol*, M. Bahrami

School of Engineering Science, Simon Fraser University, BC, Canada

ARTICLE INFO

Article history:

Received 22 December 2010

Received in revised form 19 February 2011

Accepted 21 February 2011

Available online 26 February 2011

Keywords:

PEM fuel cell

Gas diffusion layer

Water permeability

Breakthrough pressure

ABSTRACT

Water transport through gas diffusion layer of proton exchange membrane fuel cells is investigated experimentally. A filtration cell is designed and the permeation threshold and the apparent water permeability of several carbon papers are investigated. Similar carbon paper with different thicknesses and different Teflon loadings are tested to study the effects of geometrical and surface properties on the water transport. Permeation threshold increases with both GDL thickness and Teflon loading. In addition, a hysteresis effect exists in GDLs and the permeation threshold reduces as the samples are retested. Moreover, several compressed GDLs are tested and the results show that compression does not affect the breakthrough pressure significantly. The measured values of apparent permeability indicate that the majority of pores in GDLs are not filled with water and the reactant access to the catalyst layer is not hindered.

© 2011 Elsevier B.V. All rights reserved.

1. Introduction

Polymer membrane electrode fuel cells (PEMFCs) have emerged as promising power sources in automotive, electronic, portables, and stationary applications [1]. PEMFCs complete an electrochemical reaction and combine hydrogen with oxygen to produce water, releasing heat and electricity which can be used for a variety of applications [2]. To have a continuous power generation, reactants should reach the catalyst layer while water is removed, simultaneously. Numerous studies in the past decade have been devoted to the investigation of transport phenomena in PEMFCs aiming to improve the overall cell performance, reliability, and durability [3–9]. In spite of these extensive studies, water transport in gas diffusion layer (GDL) has remained an unresolved issue. Hydrophilic GDLs will lead to membrane dehydration and blockage of the pores and as a result hindering of reactant access to catalyst layers [10]. To prevent these issues, the GDL is commonly treated with polytetrafluoroethylene (PTFE). However, this could lead to water flooding especially in high power densities; flooding is a result of continuous generation of water in the cathode side and the hydrophobicity of the GDL which avoids water permeation. Therefore, an in-depth knowledge of the onset of water permeation and the apparent water permeability of GDLs is valuable and

help researchers to design modified GDLs for a more efficient water management.

Effects of PTFE content, GDL thickness, and existence of microporous layers on the overall cell performance are investigated extensively in the literature, see for example [10–15]. However, several parameters are involved in the performance of an actual fuel cell; this prevents clear understanding of the effect of water transport through GDL on the overall cell performance. Dai et al. [16] investigated the effects of PTFE content on the liquid and vapor water transport through GDLs subjected to various reactant humidities and temperatures. They found out that the flooding problem was also affected by the air stream properties and temperature.

Hydrophobicity prevents water transport through dry GDL. The accumulated water will then be absorbed into the membrane causing the membrane to swell. The swelled membrane pressurizes the GDL until the breakthrough pressure is achieved where water will be pushed through the GDL pores. Benziger et al. [17] were among the first groups who directly measured the permeation properties of GDLs. They investigated the effect of PTFE loading on the permeation threshold and apparent permeability. They mentioned that water permeates through the largest pores of the GDL. In a similar work Chou et al. [18] measured the permeation threshold and the permeability of a carbon cloth with different Teflon coatings. However, the observed trends in Chou et al.'s [18] experiment were different from the results reported by Benziger et al. [17]. Chou et al. [18] related the water permeation properties to pore size distribution of GDL rather than surface behavior properties of the fibers.

* Corresponding author at: Mechatronic Systems Engineering, Simon Fraser University, # 4300, 250-13450 102nd Avenue, Surrey, BC, Canada V3T0A3. Tel.: +1 778 782 8587; fax: +1 778 782 7514.

E-mail addresses: ata42@sfu.ca, ali.tamayol@sfu.ca (A. Tamayol).

Nomenclature

A	GDL area (m)
d	Pore diameter (m)
GDL	Gas diffusion layer
K	Viscous permeability (m^2)
P	Hydrostatic pressure (Pa)
P_c	Breakthrough pressure (Pa)
$P_c(0)$	Breakthrough pressure for non PTFE-treated GDL (Pa)
P_{c1}	Breakthrough pressure for an initially dry GDL (Pa)
P_{c2}	Breakthrough pressure for a dried GDL (Pa)
P_{th}	Threshold pressure for a pore (Pa)
PTFE	Polytetrafluoroethylene
Q	Volumetric flow rate ($\text{m}^3 \text{s}^{-1}$)
w	PTFE content in percentage

Greek symbols

γ	Surface tension (N m^{-1})
μ	Fluid viscosity (N s m^{-2})
θ	Contact angle

Our literature review revealed that the experimental studies on water permeation through commercial GDLs have mostly focused on the effects of PTFE contents and hydrophobicity and less attention has been paid to the effects of geometrical parameters such as GDL's thickness and porosity/compression. As such, the objectives of the present study are to:

- Investigate the effects of GDL's geometrical parameters such as thickness and porosity/compression on water permeation.
- Study the potential hysteresis effect on the permeation threshold.
- Measure the apparent water permeability of GDL to evaluate the importance of pore geometry and fiber surface behavior on the water transport properties.

A filtration cell is designed and several compressed and uncompressed Toray carbon papers of various thicknesses and PTFE contents are tested. In addition, to investigate the importance of GDL hydrophobicity on the apparent permeability, permeation tests are also repeated using a vegetable oil.

2. Experimental approach

The tested GDLs were purchased from Toray as Teflon treated carbon papers with different thicknesses. As a result of their similar production procedure, despite the different thicknesses, TGP 60, 90, and 120 have a similar microstructure. TGP 60 was obtained with 0, 5, and 20% PTFE loading while the rest of the samples have a 5% PTFE content. Fig. 1 shows a SEM image of TGP 90. The carbon papers were cut into circular samples of 2 cm diameter for the experiments.

In real PEM fuel cell operation, the compression on the GDL is not uniform. The areas under the bipolar plates' ribs are under pressure while the strips under the gas channels are not compressed. To cover both cases, in this study the breakthrough pressure has been investigated for both un-compressed and compressed samples. To investigate the compression effects, GDL samples were compressed using a hydraulic system for 20 min and then their new thickness was measured. Our thickness measurements did not show any change after the compression load was released. Therefore, one can conclude that the deformations were predominantly plastic. As a result, conducting the experiments *in situ* would not considerably change the results observed.

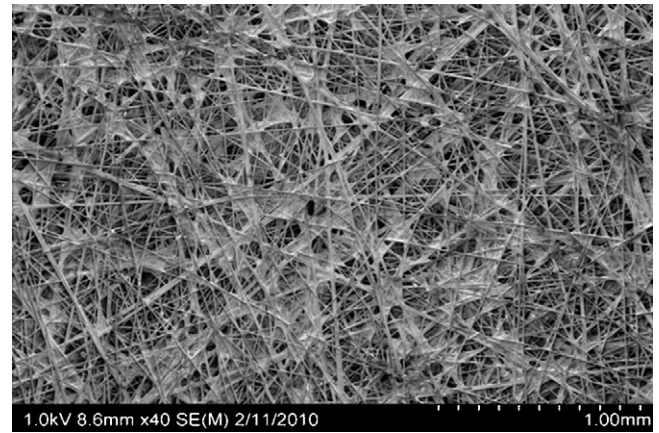


Fig. 1. A SEM image of TGP 90 with 5% PTFE content.

Table 1

Physical properties of different TGP carbon papers used in the present study; geometric properties provided by manufacturer, air permeability reported by others [4,6].

GDL	Thickness (μm)	Porosity	Air permeability (m^2)	Bulk density (g cm^{-3})
TGP 60	190	0.78	–	0.44
TGP 90	280	0.78	8.9×10^{-12} [4]	0.45
TGP 120	370	0.78	8.7×10^{-12} [6]	0.45

The properties of the tested materials are summarized in Table 1. Distilled water was used as the working fluid in the majority of the tests. In addition, TGP 120 was tested using a vegetable oil of density and viscosity of 908 kg m^{-3} and 0.071 N s m^{-2} , respectively.

A custom-built pressurized membrane filtration cell was used for measuring the water permeation properties, as shown in Fig. 2. The cell was made up of an acrylic tube of 1.25 cm diameter and 1 m height. The samples were sandwiched between two acrylic flanges and the circular opening area of the cell on top of the sample was 1 cm in diameter. A syringe pump (Harvard Apparatus, QC, Canada)

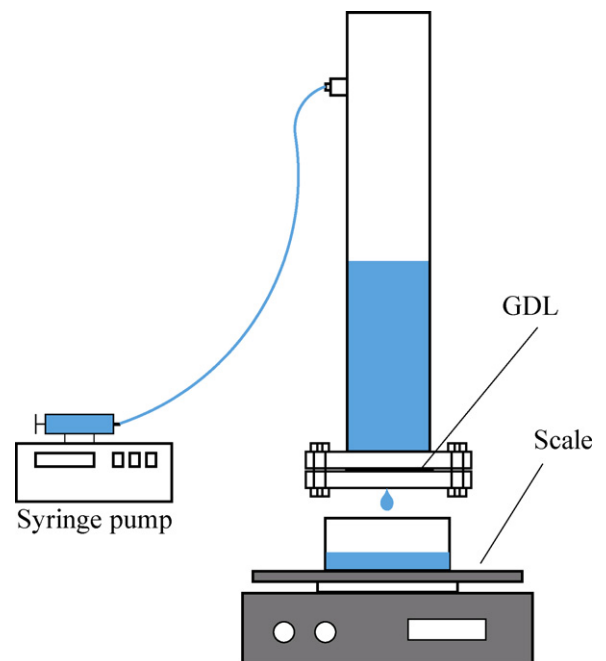


Fig. 2. Schematic representation of the designed test setup.

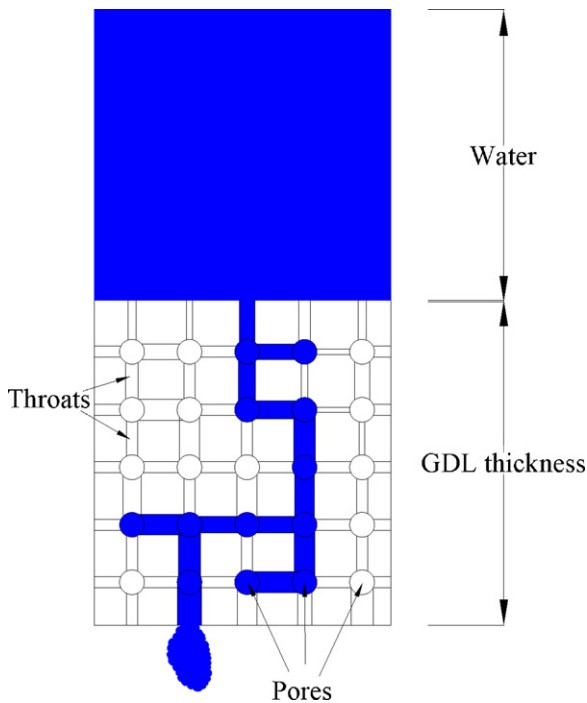


Fig. 3. Geometrical model representing water transport through GDL.

was feeding the system with a controlled flow rate with 0.5% accuracy. For testing the permeation threshold, water was fed with the flow rate of 2 ml min^{-1} . The water column on top of the GDL was associated with the applied hydrostatic pressure. The onset of the permeation threshold was considered as the pressure that led to water flow commenced, P_{c1} . Since water is generated constantly in operating fuel cells, the flow rate was kept constant and the maximum height representing the maximum pressure was recorded. The tested GDL was then removed and dried using a heater for 4 h to make sure that all the water was dried. The drying temperature was kept below 70°C to minimize the possibility of Teflon flowing that might affect the microstructure [17]. Then, the dried samples were tested again using the filtration cell and the new permeation thresholds, P_{c2} , were determined. To investigate the hysteresis effect on the permeation threshold the same approach was repeated several times. In addition, few compressed samples were also tested and the first and second trial breakthrough pressures were determined.

To calculate the apparent permeability, the water level was kept constant using the syringe pump and the flow rate passing the sample was measured. The bulk flow was calculated using a precision scale by weighting the collected test fluid over a set period of time. Moreover, to investigate the saturation of GDLs, a similar experiment was carried out using the vegetable oil.

3. Water permeation analysis

Following [19–22] GDL can be modeled as a network of pore connected by throats together. The fluids (air and water) are stored in the pores, while the volume occupied by throats is zero. The water transport resistance is associated with the throats and pores do not apply any resistance against the flow [23]. A schematic representation of such a two-dimensional network with each pore connected to four throats and a diagram of water penetration through GDL is depicted in Fig. 3. In this model, the pores are non-uniformly distributed. As a result, water travels a tortuous path through a limited number of pores, see Fig. 3. The breakthrough pressure for a pore of diameter d is related to the minimum distance of the fibers and

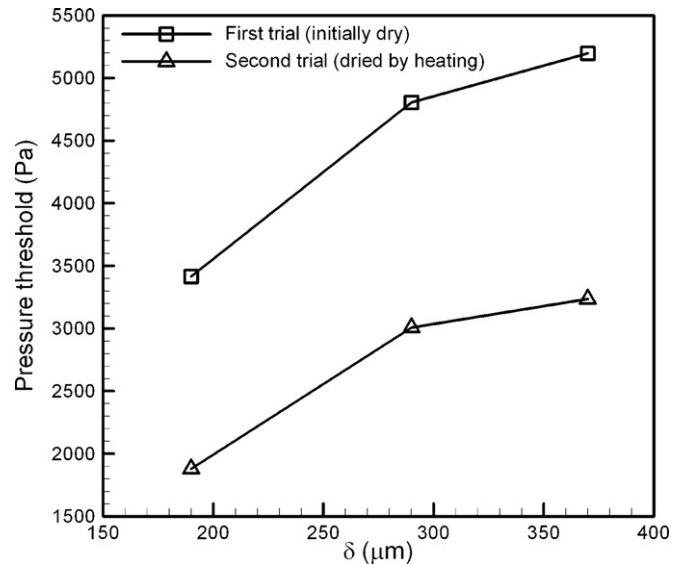


Fig. 4. Effect of GDL thickness with 5% PTFE loading on the breakthrough pressure.

can be described by the Young and Laplace relationship [24]:

$$-P_{th} = \frac{4\gamma \cos \theta}{d} \quad (1)$$

where γ is the surface tension of water, θ is the contact angle of water with the pore surface. Water cannot penetrate the pore unless the applied pressure is larger than P_{th} . Once water commences to flow, the volumetric flow rate passing GDL is related to the applied pressure, pore size distribution, and the medium saturation. Apparent permeability, K , can be used as a measure for the ability of the porous GDL to pass water [25]:

$$\frac{P}{\delta} = \frac{\mu Q}{K A} \quad (2)$$

where μ is the fluid viscosity, A is the GDL area, δ is the GDL thickness, P is the applied hydrostatic pressure which is related to the height of water column in the permeation cell, Q is the volumetric flow rate of water, and K is the permeability which can be interpreted as the flow conductance of GDLs [26].

4. Results and discussion

4.1. Permeation threshold (breakthrough pressure)

To determine the permeation breakthrough pressure, water was added slowly, 2 ml min^{-1} , to minimize the flow induced vibration. Once the water column height reached the threshold, water started to flow from the sample. The pressure values associated with this height are reported in Table 2.

The reported data in Table 2 are the average values for at least 3 different samples from the same carbon paper sheet. It was observed that when the water supply was disconnected, the water flow continued until almost the entire water column was drained. Moreover, it was observed that in a constant pressure head, the flow rate increased by time till a steady condition was reached. In an actual fuel cell, water is produced constantly. As such, in this experiment the flow rate of 2 ml min^{-1} was maintained and the maximum pressure, P_{max} , was recorded. To investigate any hysteresis effects, the tested samples were dried as described previously. The same experiment is then repeated on the dried GDLs, the average values of the permeation threshold are listed in Table 2.

The measured values for the permeation threshold are plotted as a function of GDL thickness in Fig. 4. It can be seen that

Table 2

The measured values for critical pressures and the maximum pressure.

GDL	δ (μm)	P_{c1} (dry GDL)	P_{max} (dry GDL)	P_{c2} (dried GDL)	PTFE loading (%)	Remarks
TGP 60	190	4527.1	4854.0	2157.3	20	Uncompressed
TGP 60	190	3415.8	3759.0	1879.5	5	Uncompressed
TGP 60	190	3407.6	3726.3	1716.1	0	Uncompressed
TGP 90	280	3783.5	4113.1	1917.6	5	Uncompressed
TGP 120	370	5197.2	5491.4	3236.0	5	Uncompressed
TGP 120	350	4952.0	5197.2	–	5	Compressed
TGP 120	320	5001.1	5393.3	3137.9	5	Compressed

thinner GDLs pass water at a lower pressure, as expected. The samples with 5% PTFE loading were dried several times and retested using the pressurized membrane test setup. The relative reduction in the permeation threshold in the first and the second trials, $(P_{c2} - P_{c1})/P_{c1}$, for all of the samples was almost similar. Interestingly, the number of trials for drying and testing more than twice did not affect our results significantly and the hysteresis effect was more pronounced in the first two trials. The reason for this hysteresis is not clearly known. However, based on previous studies, surface degradation, microstructural deformation, and existence of nano-size water droplets are the main reasons for changes in the water permeation properties of GDL [17].

Both Chou et al. [18] and Benziger et al. [17] modeled GDL as a single layer of parallel microchannels with different diameters. As such, they argued that the water transport properties are influenced by the dimensions of the channel with the maximum diameter. Based on their model and using our experimental results for the breakthrough pressure, it can be concluded that the maximum pore diameter is reduced by increasing the GDL thickness. However, all the GDLs tested here have the same production procedure and it is expected to have similar microstructure. It should be noted that air permeability is the property that should be used to comment on the porous medium microstructure. The air permeability values, listed in Table 1, confirm the similarity of the microstructures. As a result, the multi layer geometrical model shown in Fig. 3 is more realistic. In this model, the length of the GDL affects the number of layers; thus, the breakthrough pressure can vary with GDL thickness.

To investigate the effect of PTFE coating on the breakthrough pressure, the present data for TGP 60 and the experimental data of Benziger et al. [17] for TGP 120 are plotted in Fig. 5. It can be seen that there is a direct relation between the onsets of water permeation and the PTFE loading. However, the flow threshold is not affected significantly both at low values of PTFE content, i.e., 5% Teflon coating and above 40% PTFE loading. Fig. 5, also indicates that for higher PTFE loadings, the relative drop in the breakthrough pressure drop for dried GDLs is larger. This shows that the surface PTFE coating was degraded by water flow and affected the water transport in GDL. In Fig. 6, the ratio between break through pressures at various PTFE contents, P_c , to that of the samples without PTFE treatment, $P_c(0)$, is plotted for the present experimental data and the results reported by Benziger et al. [17]. It can be seen that both experiments follow similar trends which can be described by the following correlation:

$$\frac{P_c}{P_c(0)} = 0.38(3.62 - e^{-0.105w}) \quad (3)$$

where w is the PTFE content in percentage.

The data reported in Table 2 for compressed GDLs did not show a significant variation in the permeation threshold. Although com-

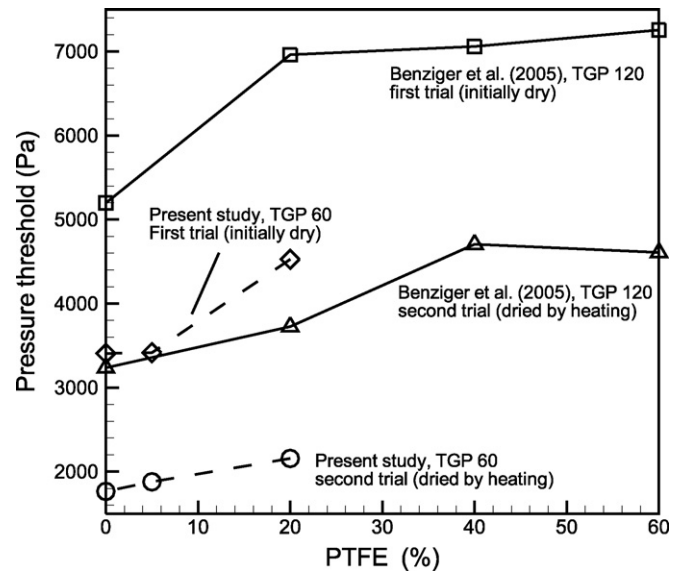


Fig. 5. Effect of PTFE loading on the breakthrough pressure in the present study and the data reported by Benziger et al. [17].

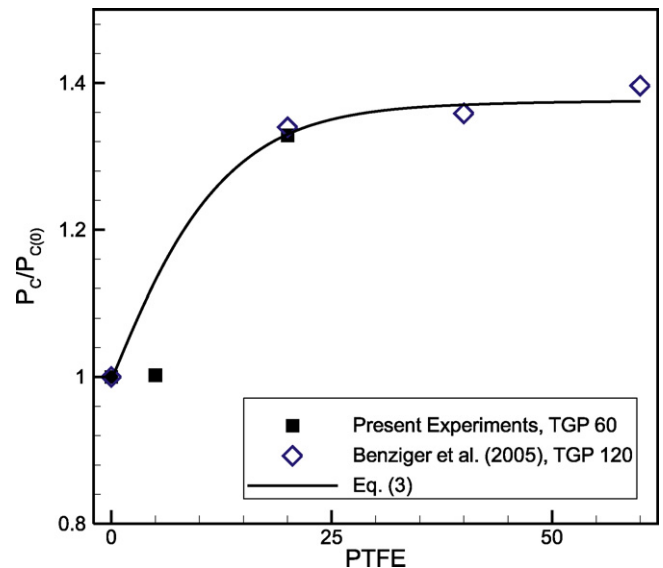


Fig. 6. The ratio between break through pressures at various PTFE contents to that of the samples without PTFE treatment, $P_c/P_c(0)$ is plotted for the present experimental data and the results reported by Benziger et al. [17].

pression reduces the average pore size of GDL, it also reduces the distance that water should penetrate and also can cause fiber fracture resulting in the occurrence of local hydrophilic spots. As such, the observed trend is reasonable.

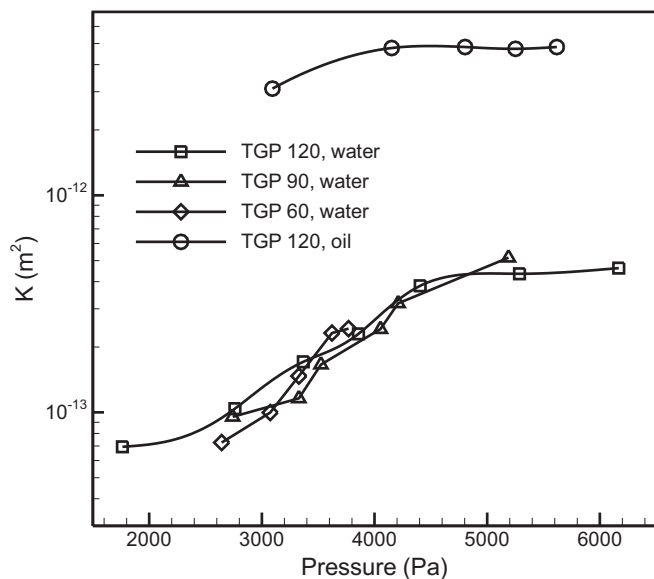


Fig. 7. Apparent permeability of 5% PTFE loading GDLs with different thicknesses.

4.2. Apparent permeability

To further investigate the effect of applied pressure drop on the water transport through GDL, the apparent permeability of samples of wet GDLs were tested. Water was fed with a controlled flow rate to the filtration cell containing a wet GDL and the steady water level was recorded as the associated pressure in Eq. (2). The effluent flow rate was also measured at the steady state condition to ensure that the inlet and outlet flow rates of the cell are identical. The flow rate was then used for calculating the permeability.

The calculated values for the apparent permeability are shown in Fig. 7. It can be seen that: (i) all carbon papers have similar apparent permeability, (ii) their permeability is not a function of their thicknesses. This is in agreement with the observed trend for the air permeability of the samples reported by others [4,6]. More importantly, the results showed a direct relationship between the applied pressure and the resulting apparent permeability. This was caused by the fact that as the applied pressure was increased more of pores were filled with water resulting in a lower resistance towards water transport.

An ideal GDL should permit water to be removed from the catalyst layer on the cathode side without hindering the reactant access to the catalyst layer. Therefore, a limited number of pores should be occupied by water, i.e., GDL should have low water saturation. A comparison between water permeability and permeability of a more wetting liquid such as the vegetable oil can be used to determine if the wetting fluid could permeate through more pores than water. In an actual fuel cell these extra pores will allow an effective reactant transport. As such, the apparent permeability of TGP 120 was determined using a vegetable oil.

The measured values of permeability were an order of magnitude higher than water permeability and still lower than air permeability (approximately $9 \times 10^{-12} \text{ m}^2$). Therefore, it can be concluded that only a limited number of pores were occupied by water and the rest of the pores allowed reactant access to the catalyst layer, i.e., GDLs have low water saturation. This is in agreement with the observations of Benziger et al. [17] through weighting wet and dry GDLs.

5. Conclusions

In the present study, a permeation cell was designed and the breakthrough pressure of several compressed and uncompressed Toray carbon papers of various thicknesses and PTFE contents were determined. The same test procedure was repeated several times to investigate any hysteresis effects on the permeation threshold. Moreover, the apparent permeability of the tested samples was measured. In addition, to investigate the importance of GDL hydrophobicity on the apparent permeability, the permeation test was repeated using a vegetable oil. The highlights of the present study can be listed as:

- The permeation threshold increased with thickness and PTFE content.
- There was a significant reduction of the permeation threshold after the first repetition.
- The apparent permeability was not a function of GDL thickness.
- The GDL hydrophobicity had a significant impact on apparent water permeability.
- Moderate compression of GDL did not affect the permeation threshold significantly.
- The majority of pores in the tested GDLs were not filled with water to hinder the reactant access to the catalyst layer.

Based on our experimental results, a thinner GDL with approximately 20% PTFE loading allows water transport in lower pressures while low water saturation is maintained. This can improve the fuel cell performance especially in high current densities. However, usually other considerations such as degradation and mechanical strength should be considered in the process of selecting the thickness of GDL in PEMFCs.

Acknowledgements

A.T. would like to thank British Columbia Innovation Council (BCIC) for BCIC Innovation Scholars Award. Financial support of Natural Sciences and Engineering Research Council of Canada, NSERC, is acknowledged by both authors.

References

- [1] A. Faghri, Z. Guo, *International Journal of Heat and Mass Transfer* 48 (19–20) (2005) 3891–3920.
- [2] J.P. Feser, A.K. Prasad, S.G. Advani, *Journal of Power Sources* 162 (2) (2006) 1226–1231.
- [3] J.G. Pharoah, *Journal of Power Sources* 144 (1) (2005) 77–82.
- [4] J.T. Gostick, M.W. Fowler, M.D. Pritzker, M.A. Ioannidis, L.M. Behra, *Journal of Power Sources* 162 (1) (2006) 228–238.
- [5] L. Cindrella, A.M. Kannan, J.F. Lin, K. Saminathan, Y. Ho, C.W. Lin, J. Wertz, *Journal of Power Sources* 194 (1) (2009) 146–160.
- [6] M.F. Mathias, J. Roth, J. Fleming, W. Lehnert, in: W. Vielstich, H.A. Gasteiger, A. Lamm (Eds.), *Handbook of Fuel Cells—Fundamentals Technology and Applications*, John Wiley & Sons, New York, 2003, pp. 517–537.
- [7] M. Prasanna, H.Y. Ha, E.A. Cho, S.A. Hong, I.H. Oh, *Journal of Power Sources* 131 (1–2) (2004) 147–154.
- [8] M.V. Williams, E. Begg, L. Bonville, H.R. Kunz, J.M. Fenton, *Journal of The Electrochemical Society* 151 (8) (2004) A1173–A1180.
- [9] A. Tamayol, M. Bahrami, *Journal of Power Sources* 196 (7) (2011) 3559–3564.
- [10] H. Li, Y. Tang, Z. Wang, Z. Shi, S. Wu, D. Song, J. Zhang, K. Fatih, J. Zhang, H. Wang, Z. Liu, R. Abouatallah, A. Mazza, *Journal of Power Sources* 178 (1) (2008) 103–117.
- [11] G.G. Park, Y.J. Sohn, T.H. Yang, Y.G. Yoon, W.Y. Lee, C.S. Kim, *Journal of Power Sources* 131 (1–2) (2004) 182–187.
- [12] G. Velayutham, J. Kaushik, N. Rajalakshmi, K.S. Dhathathreyan, *Fuel Cells* 7 (4) (2007) 314–318.
- [13] J. Ihonen, M. Mikkola, G. Lindbergh, *Journal of The Electrochemical Society* 151 (8) (2004) A1152–A1161.
- [14] K. Tüber, D. Póca, C. Hebling, *Journal of Power Sources* 124 (2) (2003) 403–414.
- [15] U. Pasaogullari, C.Y. Wang, *Journal of The Electrochemical Society* 151 (3) (2004) A399–A406.
- [16] W. Dai, H. Wang, X.Z. Yuan, J.J. Martin, Z. Luo, M. Pan, *Journal of Power Sources* 185 (2) (2008) 1267–1271.

- [17] J. Benziger, J. Nehlsen, D. Blackwell, T. Brennan, J. Itescu, *Journal of Membrane Science* 261 (1–2) (2005) 98–106.
- [18] Y.I. Chou, Z.Y. Siao, Y.F. Chen, L.Y. Sung, W.M. Yang, C.C. Wang, *Journal of Power Sources* 195 (2) (2010) 536–540.
- [19] A. Bazylak, V. Berejnov, B. Markicevic, D. Sinton, N. Djilali, *Electrochimica Acta* 53 (26) (2008) 7630–7637.
- [20] B. Markicevic, A. Bazylak, N. Djilali, *Journal of Power Sources* 171 (2) (2007) 706–717.
- [21] O. Chapuis, M. Prat, M. Quintard, E. Chane-Kane, O. Guillot, N. Mayer, *Journal of Power Sources* 178 (1) (2008) 258–268.
- [22] P.K. Sinha, C.Y. Wang, *Electrochimica Acta* 52 (28) (2007) 7936–7945.
- [23] F.A.L. Dullien, *Porous Media: Fluid Transport and Pore Structure*, 2nd ed., Academic Press, New York, 1992.
- [24] H.J. Butt, K. Graf, M. Kappl, *Physics and Chemistry of Interfaces*, Wiley-VCH, Weinheim, 2006.
- [25] A. Tamayol, M. Bahrami, *International Journal of Heat and Mass Transfer* 52 (9–10) (2009) 2407–2414.
- [26] A. Tamayol, M. Bahrami, *Physical Review E* (2010).